Received: 6 February 2024 | Revised: 3 April 2024 | Accepted: 9 April 2024

DOI: 10.1111/ppl.14306

ORIGINAL RESEARCH

Physiologia Plantarum

ChloroSpec: A new *in vivo* chlorophyll fluorescence spectrometer for simultaneous wavelength- and time-resolved detection

Sanchali Nanda[1] | Tatyana Shutova[1] | Maximiliano Cainzos[1] | Chen Hu[2] | Bart Sasbrink[2] | Pushan Bag[3] | Tristan den Blanken[4] | Ronald Buijs[4] | Lex van der Gracht[4] | Frans Hendriks[4] | Petar Lambrev[5] | Rob Limburg[4] | Vincenzo Mascoli[2] | Wojciech J Nawrocki[2] | Michael Reus[5] | Ramon Parmessar[4] | Björn Singerling[4] | Ivo H M Stokkum[2] | Stefan Jansson[1] | Alfred R. Holzwarth[2,5,6]

[1]Umeå Plant Science Centre, Department of Plant Physiology, Umeå University, Umeå, Sweden

[2]Biophysics of Photosynthesis, Department of Physics and Astronomy, Faculty of Science, Vrije Universiteit Amsterdam, The Netherlands

[3]Section of Molecular Plant Biology, Department of Biology, Oxford University, Oxford, United Kingdom

[4]Technology Centre, Vrije Universiteit Amsterdam, The Netherlands

[5]Max-Planck-Institute for Chemical Energy Conversion, Mülheim a.d. Ruhr, Germany

[6]ChloroSpec B.V., De Boelelaan 1105, 1081 HV Amsterdam, The Netherlands

Correspondence
Stefan Jansson,
Email: stefan.jansson@umu.se

Funding information
Demonstrator lab Amsterdam; the Dutch Organization for Scientific Research; Kempestiftelserna; Vetenskapsrådet; Knut och Alice Wallenbergs Stiftelse; Stiftelsen för Strategisk Forskning; Human Frontier Science Program

Edited by W. Schröder

Abstract

Chlorophyll fluorescence is a ubiquitous tool in basic and applied plant science research. Various standard commercial instruments are available for characterization of photosynthetic material like leaves or microalgae, most of which integrate the overall fluorescence signals above a certain cut-off wavelength. However, wavelength-resolved (fluorescence signals appearing at different wavelengths having different time dependent decay) signals contain vast information required to decompose complex signals and processes into their underlying components that can untangle the photophysiological process of photosynthesis. Hence, to address this we describe an advanced chlorophyll fluorescence spectrometer - *ChloroSpec* - allowing three-dimensional simultaneous detection of fluorescence intensities at different wavelengths in a time-resolved manner. We demonstrate for a variety of typical examples that most of the generally used fluorescence parameters are strongly wavelength dependent. This indicates a pronounced heterogeneity and a highly dynamic nature of the thylakoid and the photosynthetic apparatus under actinic illumination. Furthermore, we provide examples of advanced global analysis procedures integrating this three-dimensional signal and relevant information extracted from them that relate to the physiological properties of the organism. This conveniently obtained broad range of data can make *ChloroSpec* a new standard tool in photosynthesis research.

1 | INTRODUCTION

Chlorophyll (Chl) fluorescence, the light emitted from the key pigments of the photosynthetic apparatus has - since the first study of the phenomenon (Kautsky and Hirsch, 1931) - provided over the last few decades fundamental insights into the functioning of the photosynthetic apparatus of green organisms (Kalaji et al., 2014, Kalaji et al., 2017). These include the characterization of the yields, rates and mechanisms of the charge/electron transfer of the primary reactions and the electron transport chain, mechanisms of photoprotective (non-photochemical

quenching-NPQ) and photoadaptive responses (Bag, 2021; Baker, 2008; Baker and Oxborough, 2004; Horton et al., 1996; Malnoë, 2018; Minagawa, 2013; Stirbet and Govindjee, 2011). The information content of Chl fluorescence has given rise to many applications in areas of plant research such as plant physiology, ecophysiology, in greenhouses and agriculture and forest research in the open field (Bąba et al., 2019; Berger et al., 2022; Gorbunov and Falkowski, 2022; Strasser et al., 2000; Sun et al., 2022; Zavafer et al., 2020). Remote detection from satellites and unmanned aerial vehicles (UAV)s relies on solar-induced Chl fluorescence (SIF) detection (Pieruschka et al., 2012; Sun et al., 2023). Chl fluorescence is also used to detect and characterize abiotic and biotic stress responses (Guidi and Degl'Innocenti, 2012) and for phenotyping during breeding/selection of new stress resistant and/or higher yielding crops or microalgae (Chaerle et al., 2009; Pérez-Bueno et al., 2019). It has also been extended to cover spatial resolution by fluorescence imaging (Johnson et al., 2009; Nedbal and Whitmarsh, 2004) which – depending on the resolution achieved - allows to differentiate between macroscopic and/or microscopic variations in the fluorescence of a leaf related to differences in Chl responses, stress conditions (Lichtenthaler, 2021; Moustakas et al., 2021) or to variations in chloroplast structure at the subcellular level (Wientjes et al., 2017).

For applications in laboratories, greenhouses and also in open field, essentially two different approaches are applied and commercial instruments have been developed by several companies for both: 1) so-called pulse-amplitude modulation (PAM) (Genty et al., 1989) and 2) direct detection (Kalaji et al., 2014). Each approach has advantages and disadvantages for different applications but a common feature in commercially available instruments is detection of a single fluorescence signal in a wavelength-integrated manner, although first attempts have been made to split the entire Chl fluorescence range into two regions (Pfündel, 2021). In general, a short-wavelength cut-off filter in front of the detector removes the excitation light and fluorescence emitted above the cut-off wavelength is integrated in the detection system (Kalaji et al., 2014, Kalaji et al., 2017). This simple wavelength-integrating measuring mode was primarily determined by the limitations of the available light detection technology when these Chl fluorometer techniques were developed. Despite the success and huge impact and growth of applications of such Chl fluorometers, this detection method largely ignores the full information content present in the wavelength-dependence of the Chl fluorescence signals. Although, emission wavelength dependence has been reported in green alga and cyanobacterial strains (Kaňa et al., 2009; Remelli and Santabarbara, 2018; Rizzo et al., 2014; Santabarbara et al., 2020, 2019), such characterisation has not been done in higher plants. The wavelength-dependence of the Chl fluorescence signals has instead been exploited in the development of ultrafast Chl fluorescence detection techniques which over the last decades have provided both time and wavelength resolution (Chukhutsina et al., 2019; Croce and van Amerongen, 2020; Gilmore and Ball, 2000; Holzwarth, 1986; Holzwarth et al., 1985, Holzwarth et al., 2009). Together with the application of advanced data analysis of the recorded signals, like e.g. global analysis and kinetic target analysis methods, this technique has provided much more detailed insights into the functioning of the photosynthetic apparatus than would be possible using single wavelength (or wavelength-integrated) methods (Beechem et al., 1985; Holzwarth, 1996; Roelofs et al., 1992; van Stokkum et al., 2004). Recording of 3-D data surfaces (intensity *vs*. time *vs*. wavelength) allows e.g. for the separation/dissection of the total signals into their sub-components based on their spectral and temporal/kinetic differences. As one recent example, we have studied dissipation mechanisms in pine needles under extreme winter stress by ultrafast time-resolved and wavelength-resolved methods (Bag et al., 2020). Despite their power, the number of published studies using such approaches in photosynthesis research are relatively few as they require expensive instruments and deep expert knowledge to operate, analyse and interpret their data. This has severely restricted their wider use in plant research and furthermore, the complexity of instrumentation restricts its usage to the laboratory.

However, optical detection technologies have in the last decade developed rapidly. This now opens up possibilities to develop a novel generation of Chl fluorometers that could extend the capabilities of the conventional Chl fluorometers – easy-to-use and wide range of applications – by adding full wavelength-resolution currently realized only in combination with high time-resolution techniques. We describe here a Chl fluorometer – *ChloroSpec* - that combines these properties. It can be used broadly in plant and microalgae research and has the capacity – in combination with user friendly advanced data analysis methods - to increase the potential of Chl fluorescence detection for gaining deeper insights into the properties of photosynthetic organisms.

Without being exhaustive in demonstrating the possibilities, we present here some typical examples of data recording and analysis by *ChloroSpec* from a wide range of plant materials; leaves, needles and micro-algae. We show that the conventionally used fluorescence parameters measured by wavelength-integrating instruments are in fact strongly wavelength dependent, indicating a pronounced heterogeneity of the photosynthetic apparatus and the underlying photochemical responses. The new measuring and analysis capabilities allows for a detailed resolution and characterization of these heterogeneities that give a deeper characterization of the photosynthetic processes and their regulation .

2 | MATERIALS AND METHODS

2.1 | Plant material

Leaves of 6 week-old *Arabidopsis thaliana* Col-0 plants were grown in the greenhouse (150–180 µmol m^{-2} s^{-1} growth light) in short day conditions (8 hr day, 22°C/16 hr night, 18°C). Needles of *Picea abies* were harvested from trees grown in the greenhouse (70–90 µmol m^{-2} s^{-1} growth light) in long day conditions (16 hr day, 22°C / 8 hr night, 18°C) and from outdoor grown 40+ year-old tree in december 2023 (-20°C at the time of harvest, referred to as winter *P. abies* here after). The needles were arranged together to form a continuous surface for measurement. Leaves of 4 month old *Populus* T89 *(Populus tremula x Populus*

tremuloides, hybrid aspen) were harvested from trees grown in long day conditions (16 hr day, 22°C/8 hr night, 18°C) in the greenhouse (70–90 µmol m^{-2} s^{-1} growth light). 1 week-old wildtype strain (CC-124) of *Chlamydomonas reinhardtii* cultures were grown under continuous light of 70 µmol m^{-2} s^{-1} at 200 rpm. The leaves of indoor grown *Monstera deliciosa* with no defined growth conditions were also used for experiments. All samples were dark adapted for 30 mins before subsequent measurements at room temperature.

2.2 | Chlorophyll fluorescence measurements

Measurements were carried out using *ChloroSpec L1*. The instrument detects chlorophyll fluorescence signals from attached or detached leaves, or suspensions of microorganisms, or preparations of isolated photosynthetic components using various exchangeable sample holders. Fluorescence signals are simultaneously detected in two ways: i) by three fast photodiode channels (– sampling rate 5 MHz – at fixed, but user-selectable, wavelengths through narrow-band (10 nm FWHM) interference filters, and ii) full spectral detection by an optical spectrometer (range 500–900 nm, gated detection with minimal gate-width 10 µsec, 2048 pixels CMOS detector, AvaSpec-ULS4096CL-EVO OEM version; readout rate ≤ 2000 spectra/s for wavelength- and time-resolved analysis) (Figure 1a, instrument layout). Results can be displayed and analysed in various ways, e.g. as fast time-resolved induction curves (from the three fast photodetectors), as wavelength-resolved spectra or as 3D (intensity *vs.* wavelength *vs.* time) surfaces (Figure 1a, data output).

Three exchangeable high-intensity LEDs can be selected for providing PSII closing pulses either with single turnover flash (STF) burst

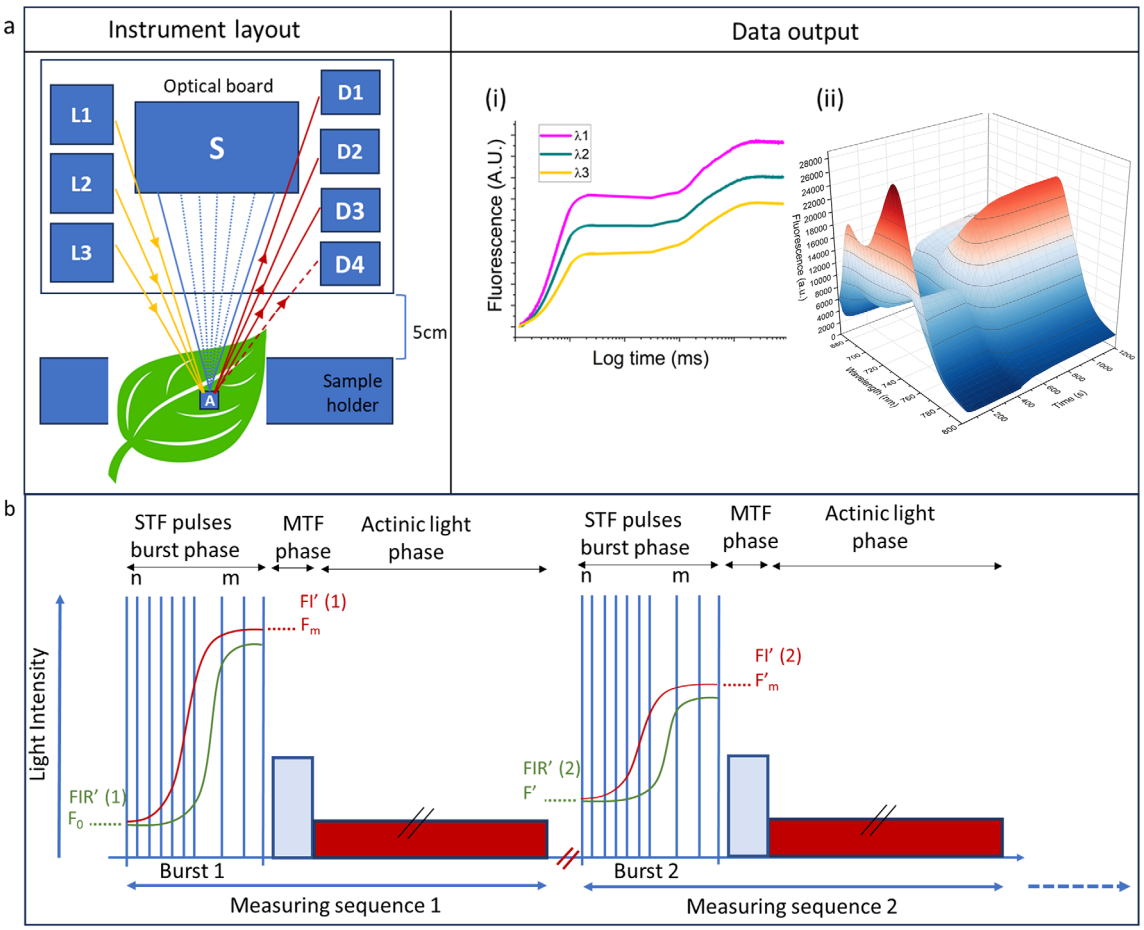

FIGURE 1 **(a)** Working principle of the instrument and a typical chlorophyll fluorescence measurement. A leaf sample is excited by one of three light emitting diode (LED) source options (L1, L2, L3) and emitted chlorophyll fluorescence is detected in two parallel ways: **(i)** three filter-photodiode combinations (D1, D2, D3) detect emitted fluorescence at three wavelengths (λ_1, λ_2, λ_3) and with a reference photodiode (D4) to give high time resolution and wavelength resolved fluorescence induction traces **(ii)** a full spectral detection by an optical spectrometer, range 500–900 nm (S) captures the emitted fluorescence yielding a 3-D representation intensity *vs.* wavelength *vs.* time. The instrument used here has L1 = red, L2 = green, L3 = infrared, D1 = 686 nm, D2 = 700 nm, D3 = 730 nm, D4 = reference.The emitted fluorescence detection area is represented as "A" on the leaf surface and is 5 mm^2 **(b)** A timing diagram of a typical measuring protocol. In measuring sequence 1, F_0 is measured from a dark-adapted leaf by a burst of single turnover (STF) pulses to attain F_m (an STF pulse consists of a 130 µsec long pulse of 60.000 µEinstein m^{-2} s^{-1} and a burst is defined as a sequence of n + m STF pulses separated by corresponding dark intervals with duration of a few msec). This is followed by a very short multi turnover flash (MTF) phase before the actinic light phase. This actinic light phase is followed by a second STF burst to measure F′ & F'_m as a function of emission wavelength. Repetition of such measuring sequences are then programmed accordingly to design any experiment of choice.

(peak intensity ≤80 000 µmol m^{-2} s^{-1}, 10–300 µsec width per pulse) or wider multi turnover flash (MTF) pulses (peak intensity ≤25 000 µmol m^{-2} s^{-1}, pulse length up to several secnds). All LEDs can be used also as actinic light sources. The standard configuration includes vis LEDs (Osram Ostar Q8WP) with peak wavelengths at 625 nm (red), 530 nm (green), and a NIR LED, peak 730 nm but can be exchanged for other wavelengths. The standard filter-photodiode wavelengths are 686, 700 and 730 nm (photodiode Hamamatsu S1227-33BR). Optionally the instrument can be equipped by a second spectrometer for special purposes like detection in the blue-green spectral region for fluorescence biosensor signals.

A typical measurement sequence consists of an initial single turnover flash (STF) burst for closing PS II RCs (fluorescence induction), a multi turnover flash (MTF) optionally followed (or preceded) by actinic light sequences, and various repetitions or modifications of such cycles (Figure 1b). Optical pulse properties such as pulse width, intensity, actinic intervals, STF and MTF closing pulses are computer-controlled and could be changed using an easy-to-use proprietary command language. In the measurements presented here a burst of STF (250 pulses, each 130 µs wide, separated by 3 ms intervals) of 60 000 µmol m^{-2} s^{-1} red excitation light was provided to a dark-adapted sample to close all PS II RCs providing the wavelength dependent fluorescence induction (FI) curves. All high precision timing for excitation pulses and detection signal gating is controlled by a Xilinx 7020 FPGA unit. The fluorescence values recorded after each pulse during an STF burst constitute the FI' curves and thereby the maximum value of the first FI' curve (FI' (1)) is the F_m. Fluorescence values are also recorded before each pulse during an STF burst to constitute FIR' curves. The first value from FI'(1)) & FIR'(1) is the F_0 (Figure 1).

From each flash the time-resolved signals (200 ns/point) at the three fixed wavelengths, as well as a full fluorescence spectrum from each pulse (30–40 µs integration window, ~2.5 nm resolution per point) was recorded. In addition the STF pulse burst was typically followed by a very short (length ≤1 ms) MTF pulse of 15 000 µmol m^{-2} s^{-1} to measure another full fluorescence spectrum defining the FI' spectrum at very high signal/noise ratio. All signals are automatically normalized to the intensity of the exciting LEDs by means of a reference photodiode. This sequence is typically followed by an actinic sequence of desired length and intensity (for NPQ studies, rapid light curves etc.), and the cycle is repeated, where FI' curves and FIR' spectra are recorded.

A standardization test of STF pulses was done to define a reasonable STF pulse duration. A range of STF pulse widths were tested; when the pulse width was longer than 70 µs the amount of variable fluorescence reached values close to 0.6, in agreement with previous studies (Figure S1) (Schansker et al., 2014; Schreiber et al., 1986).

2.3 | Spectro-kinetic data analysis

Decomposition of the NPQ spectral components/kinetics was performed by global target analysis methods on the basis of testing a variety of pseudo-first order differential equation models (Holzwarth, 1996; van Stokkum et al., 2004) applying the variable projection algorithm as the non-linear solver (Golub and Pereyra, 2003). The mathematical fit quality was checked in a standard way using residual plots and minimal χ^2-values (Holzwarth, 1996). In such multi-component fitting procedures "physically reasonable" constraints are applied to the fitting parameters. Examples of such "physically reasonable" constraints are 1) application of non-negativity constraints for spectra and concentration values, 2) unimodality (single maximum) of spectra (where it applies) and/or concentration profiles, 3) closure (in chemical systems the sum of concentrations of components can often be assumed to be constant over time) or 4) other constraints like local rank and selectivity e.g. using information from certain parts of the experiment such as concentrations at the start should be zero, are otherwise known, or are constant. In the analysis described here we have applied the non-negativity of spectra and concentrations constraints and in some cases also closure and selectivity constraints.

3 | RESULTS

3.1 | Wavelength dependent FI curves

Figure 2 shows a comparison of FI curves for dark-adapted leaves from *A. thaliana* using either a conventional Chl fluorescence instrument (Dual PAM, Walz), or the wavelength-resolving ChloroSpec L1 instrument. The FI curves in ChloroSpec are measured using a burst of short STF pulses followed by an MTF pulse (see methods) in contrast to the use of only MTF pulses in PAM. The STF closing pulse technique bears some similarity to the one used in the fast repetition rate (FRR) fluorescence instrument (Kolber et al. 1998) although there typically a much larger number of very low intensity pulses – combined also in a pulse burst – are used. A key difference is however on the detection side; in ChloroSpec fluorescence is detected in a wavelength-resolved manner while in the FRR spectrometer it is detected as a single wavelength-integrated signal (Kolber et al. 1998). Moreover, additional information about the initial rise (0.01 ms – 0.14 ms) in FI' is possible using STF bursts in ChloroSpec.

Figure 3 shows fast FI curves from dark-adapted samples measured during an STF pulse burst (c.f. Figure 1b) for *A.thaliana* and *P. abies*. The full signal is plotted for the first pulse while only the last FI' and the first FIR' data point is plotted in the subsequent STF pulses in a burst. The maximum peak (F_m) attained in FI' curves, decayed for *P. abies* while remained constant for *A. thaliana* and also for other plant species (Figure S3). The peak and decline in FI' curves implies that F_m is reached before the end of the applied STF burst sequence, and thus in shorter time in *P.abies* than in the other species. FI' curves for *C. reinhardtii* and winter *P.abies* overlap while in the other species curves differ (Figure S3). In addition to wavelength dependent distinction among FI' curves (Figure 3a-c), maximal PS II quantum yields, i.e. $F_v/F_m = (F_m\text{-}F_0)/F_m$, are strongly wavelength dependent (Figure 3d), with values ranging from 0.61 to 0.86. Typically higher F_v/F_m values are observed at 686 than at 730 nm (Figure 3d) for *A. thaliana and P. abies*. Current commercial Chl fluorescence

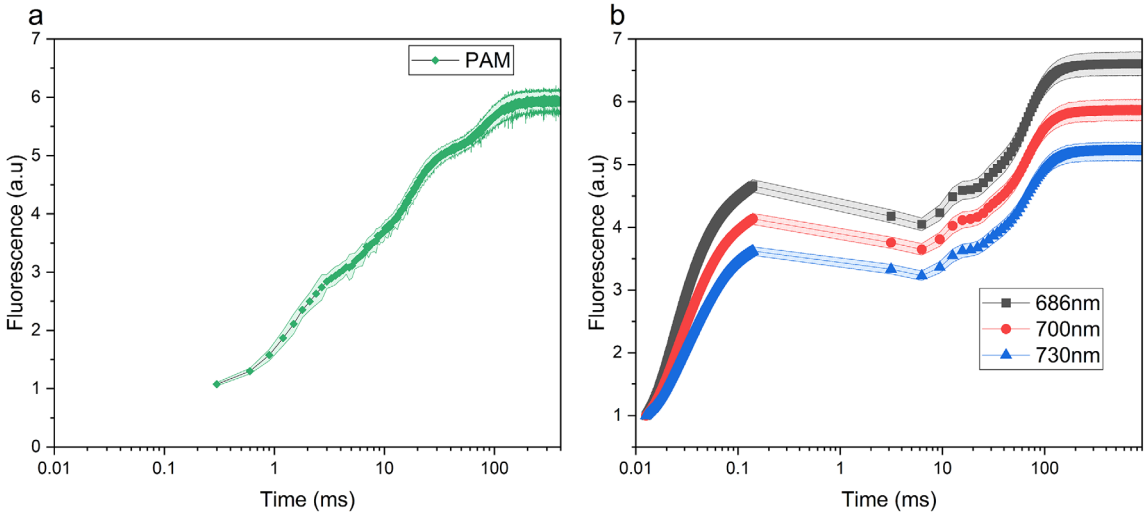

FIGURE 2 Fluorescence trace of a typical saturation pulse on a *A. thaliana* leaf in (a) PAM, consists MTF & (b) ChloroSpec, consists STF. The fluorescence values recorded after each pulse during an STF burst (FI' curves) at three different wavelength (686 nm, 700 nm and 730 nm) are depicted on the Figure 2(b). Means ± SE for n = 9.

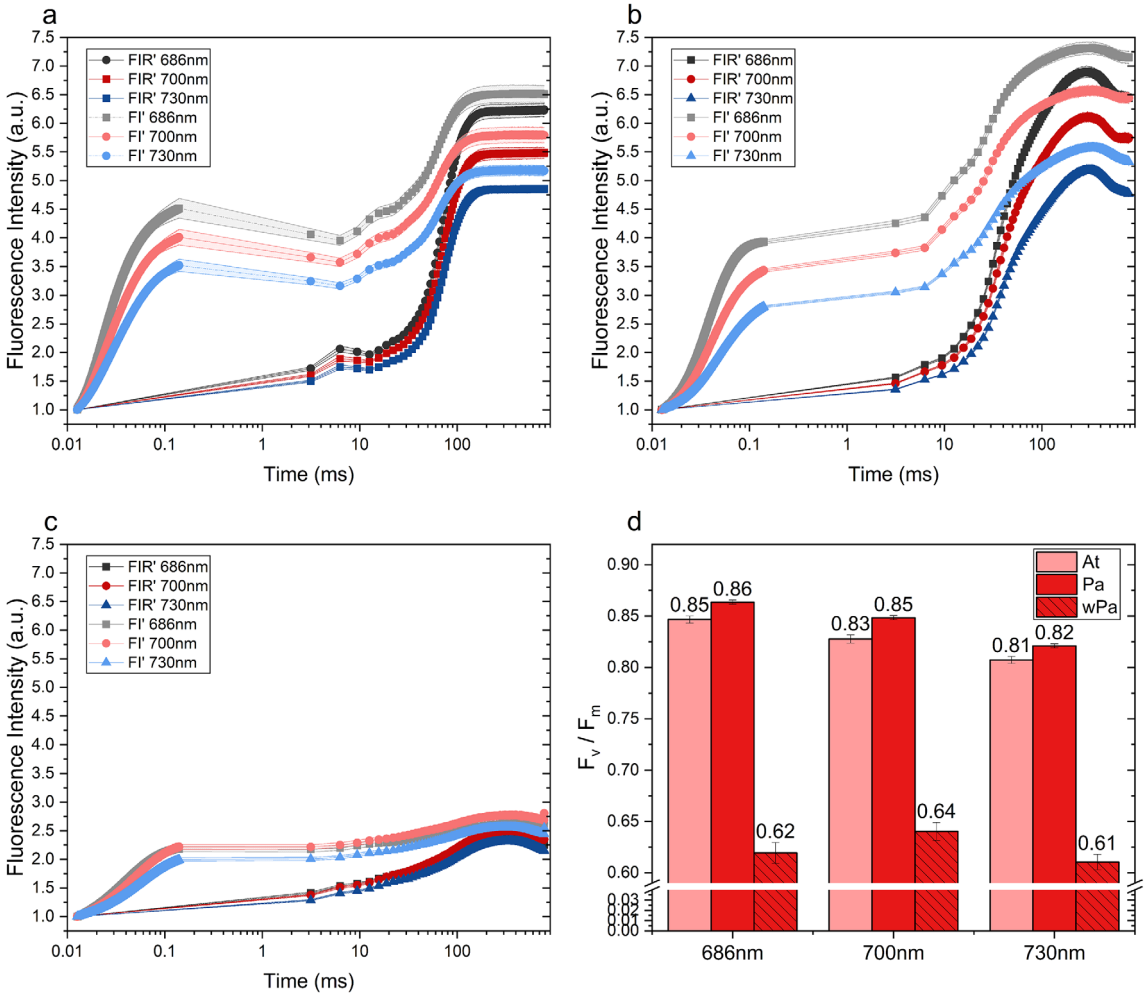

FIGURE 3 Fluorescence induction curves normalised to the first timepoint tracing evolution of FIR' and FI' in **(a)** *A. thaliana* (At) leaves **(b)** *P. abies* (Pa) needles and **(c)** winter *P.abies* (wPa) with red excitation light during the first STF burst phase of samples. **(d)** F_v/F_m of At leaves and Pa needles with red excitation light. The data is resolved at 686 nm, 700 nm and 730 nm. Means ± SE for n = 4–6.

spectrometers record only one fluorescence signal wavelength-integrated above ca. 700 nm, providing peak sensitivity around 730 nm. They therefore highly weigh the very red part of the spectrum (>700 nm), Figure 3 shows that this measurement regime substantially underestimates the actual maximal PS II yields which are highest in the 680–700 nm range. F_v/F_m values obtained by instruments like the Dual PAM (Figure S2) closely correspond to values obtained by *ChloroSpec* between 700 nm and 730 nm while F_v/F_m values at 686 nm are typically higher.

In other conditions these patterns may be different; in winter *P. abies* the 700 nm contribution to F_v/F_m (0.64) is higher compared to 686 nm. The winter needles are strongly quenched with F_v/F_m ranging between 0.61 and 0.64 while the summer needles have normal values between 0.82 and 0.86 (Figure 3d). Obviously this wavelength dependency of FI is lost in this highly quenched system (Figure 3b–c).

Figure 3a-3d, besides showing "standard" FI' curves (Kalaji et al., 2017, 2014), depicts a second set of induction curves that we hereafter call FIR' (fluorescence induction redox state dependent) curves. They represent a new type of FI curves that can not be recorded by conventional fluorescence spectrometers. With *ChloroSpec* the FI curves are recorded using a burst of STF pulses, separated by 2–4 ms dark intervals. In these short dark intervals between pulses PS II fluorescence relaxes from the previously attained FI'(n) value (maximal fluorescence yield at any given STF during a FI) at the end of a STF pulse to an FIR'(n) level at the start of the next STF pulse of the burst (minimal fluorescence yield at any given STF during a FIR). Connecting the FIR' values of all pulses of the burst gives the FIR' induction curve shown in Figure 3a-c and Figure S3. These FIR' induction curves follow a different time development compared to the corresponding conventional FI' induction curves. The reason for this behaviour is given by the progressing secondary electron transfer reactions during the dark intervals. During the STF burst pulses, the reduction of electron carriers upstream PSII will lead to a PSII acceptor side limitation and therefore a decrease in the rate of Qa oxidation by Qb. In this way, the FIR'(n) signal, and in particular the difference function of the FI'(n) signal to the FIR'(n + 1) signal can provide additional information for the characterization of the secondary electron transport processes and in particular about the reoxidation kinetics of the electron transfer chain leading to (partial) reopening of the PS II reaction centers (RCs). Note also that FIR' induction curves show pronounced wavelength dependencies, new analysis methods will however have to be developed to deduce information on the secondary electron transfer steps and their heterogeneities from the FIR' curves.

3.2 | Wavelength-dependent NPQ measurements

Wavelength-resolved fluorescence can also provide insights into the underlying mechanisms behind NPQ induction and relaxation. Figure 4a shows NPQ induction and relaxation signals for *A. thaliana* and *P. abies*. The NPQ values are higher in *P.abies* (2.5–5) with maximum values at 686 nm for both plant species. The differences are less pronounced between 700 and 730 nm in *A. thaliana* with NPQ values ranging between 1.5–2. The 3D surface for FI' (*vs.* actinic time and detection wavelength) for NPQ induction and relaxation is shown in Figure 4b. The evolution of FI' spectra during the actinic phase is presented in Figure 4c–d. The decrease in fluorescence intensity and change in spectral characteristics with time are evident. This FI' spectra allows for calculation of the "NPQ spectra" shown in Figure 4e–f; where the pronounced wavelength dependence of the NPQ signals is notable. Typically higher NPQ values around 680–690 nm and a dip with lower NPQ values around 710–730 nm is observed at the end of actinic light phase. The exact shape of that "NPQ spectrum" depends strongly on the species, genotype, growth conditions and pretreatment among other factors. The dominant 686 nm peak observed in *P.abies* is lost in the corresponding winter samples, demonstrating the effect of growth conditions on NPQ spectra as well as NPQ induction (Figures 4f and S4c). This wavelength dependence of the NPQ signals and kinetics contains decisive information for gaining deeper insight into the mechanisms and kinetics of the underlying heterogeneous NPQ processes than is possible on the basis of wavelength-integrated signals.

3.3 | A five-component kinetic model is required to describe NPQ

Clearly, the FI'(t, λ) surfaces (Figure 4c–d) lend themselves to application of advanced spectro-kinetic data analysis methods resolving temporal and spectral contributions underlying NPQ giving detailed insights into heterogeneous NPQ mechanisms. For reasons discussed previously (Holzwarth et al., 2013) we do not kinetically analyse the actual converted NPQ signals but the original FI' (t, λ) signals measured during the NPQ induction and relaxation phases. A workflow of spectro-kinetic analysis on FI' spectra is described in Figure 5a. The analysis starts by hypothesising a kinetic model followed by testing and evaluation until a best fit model is achieved (see methods for further details). The progressive testing of kinetic models for FI' spectra obtained from *A. thaliana* in Figure 4a was done as follows. A 2 component model had extremely high χ^2 value (465.15, Figure S5a) and therefore addition of components was considered in a linear kinetic scheme. The successive addition of components up to a total of 4 improved the fit and decreased the χ^2 values (Figure S5b-c). Subsequent evaluation of emission spectra (Figure S5c (i)) and time dependent concentration profiles (Figure S5c (ii) revealed the problem of unsaturating concentration of component 4 and thereby an addition of fifth component was necessary. Adding it to a linear scheme did not improve the concetration profiles, components 3–5 had not attained stable concentrations by the end of the NPQ induction phase (Figure S5d (ii)). Therefore a split reaction was added to component 2 to achieve the best fit kinetic model for *A. thaliana* (Figure 5d). The resulting components of the model represent chlorophyll fluorescent species and hence will be referred to as "species" here after. While species 1 to 4 have distinct peaks at around 690 nm and 740 nm, species 5 has a characteristic peak at 740 nm (Figure 5b). The concentration profiles indicate a stable existence of species 3 and 5 at the end of NPQ induction implying its significance

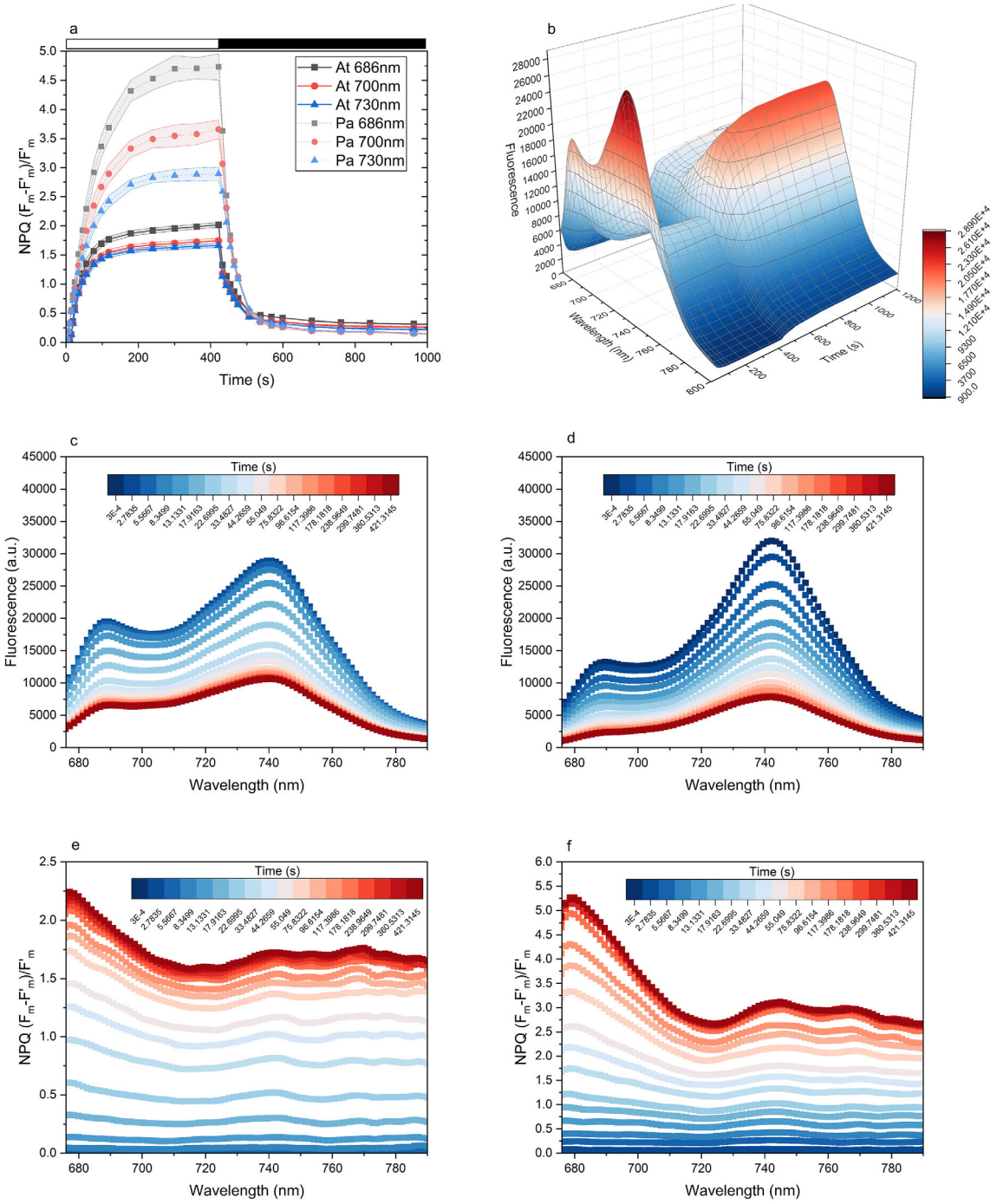

FIGURE 4 **(a)** NPQ induction (white bar) and relaxation (dark bar) kinetics of *A. thaliana* (At) leaves and *P. abies* (Pa) summer needles using 800 µmol m^{-2} s^{-1} red actinic light. The data is presented at 686 nm, 700 nm and 730 nm. Means ±SE for n = 3. **(b)** 3D spectra plot of fluorescence decrease (NPQ induction) & increase (NPQ relaxation) vs wavelength (670 nm – 800 nm) and time (s) of a *A. thaliana* leaf. 2D Fl' spectra of **(c)** At and **(d)** Pa and NPQ spectra of **(e)** At and **(f)** Pa during the actinic phase of NPQ kinetics from the data acquired in **(a)**.

for the process (Figure 5c). There is also another important property linked to the fluorescence emission spectra; the area under the spectra is proportional to their relative fluorescence quantum yield of the species. Therefore, species 1 and 2 are the most, and species 5 is the least fluorescent species or in other words; species 5 is the most quenched.

A similar five-component kinetic scheme was the result for the spectro-kinetic analysis of Fl' spectra of *P. abies* (Figure S6). The samples have a less dominant peak at around 690 nm in contrast to *A. thaliana* and species 5 has a characteristic broad shoulder peak at 740 nm (Figure S6 (i) a). Moreover, species 5 in *P.abies* has a higher concentration than species 3 in contrast to *A. thaliana* at the end of the NPQ induction phase (Figure S6 (i)-(ii) b). The area under the spectra of species 1 spectra is higher than species 2 in *P. abies* (Figure S6 (i) a) in contrast to *A.thaliana* and winter *P.abies*. The effect of stressful

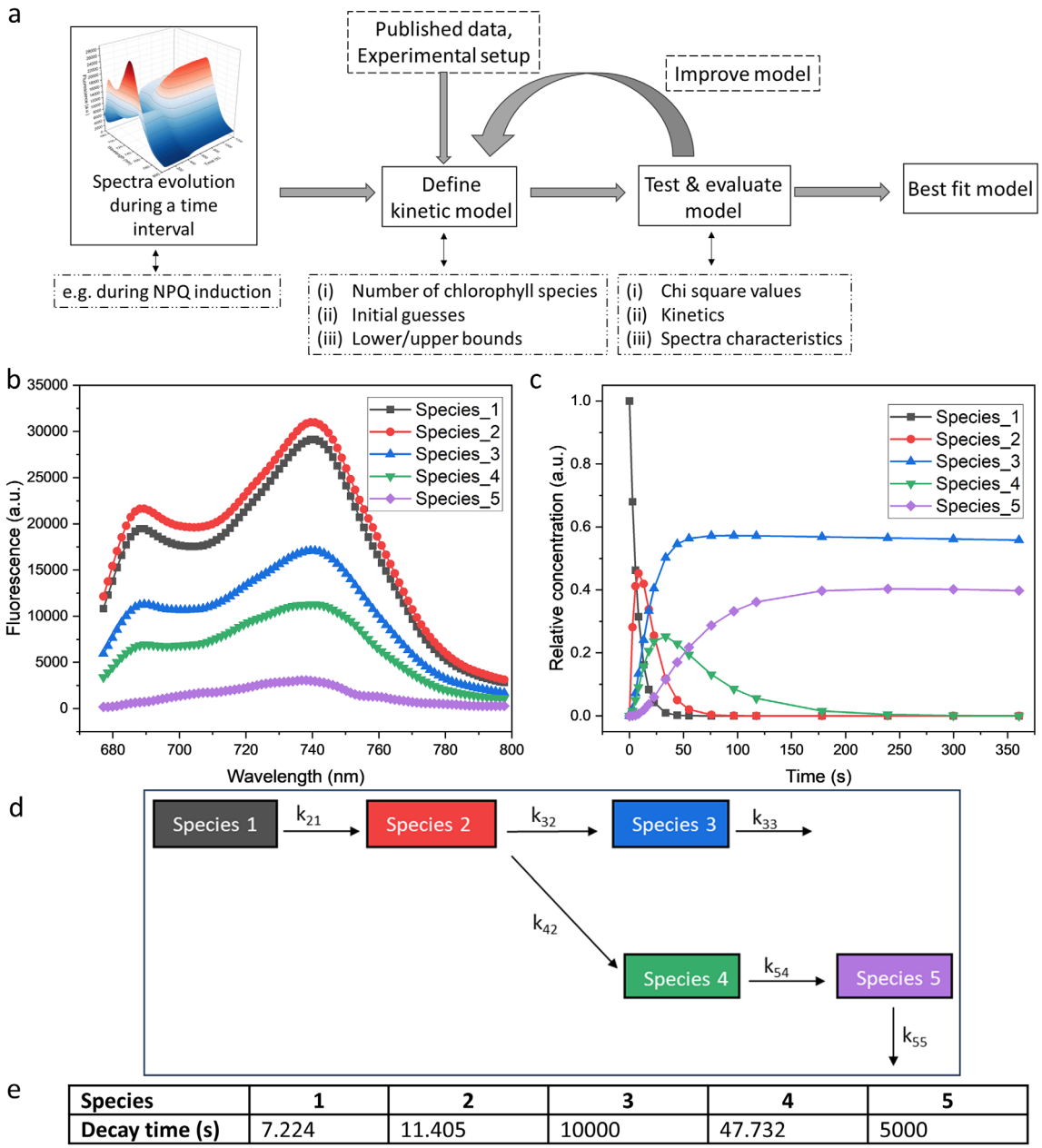

e

Species	1	2	3	4	5
Decay time (s)	7.224	11.405	10000	47.732	5000

FIGURE 5 **(a)** Work flow of kinetic target analysis. Results of decomposition of the spectra of NPQ fluorescence data by spectro-kinetic analysis (target analysis) into five component spectra and their time-dependent concentrations are presented in **(b)** & **(c)** for *A. thaliana*. Species 1 is the spectrum of the dark adapted state. The other spectra represent intermediate and end states. The resulting kinetic scheme is described in **(d)** and corresponding decay times in **(e)** with total $\chi^2 = 1.757$ for this model fit. NPQ induction kinetics data was acquired from a *A. thaliana* leaf with 800 µmol m^{-2} s^{-1} red actinic light.

winter conditions become apparent in the spectro-kinetic analysis of *P.abies*. The fluorescence intensity drops in the spectra profile and broad distinction among the 5 spectra is lost. The broad shoulder peak at 740 nm of species 5 also disappears in winter *P.abies* (Figure S6 (ii)). Normalised plots of the five component spectra at 740 nm simplify the comparison of the spectral shapes of the different species (Figure S7). These differences already suggest underlying variation in properties of chlorophyll fluorescent components/complexes in action during NPQ in different plant species.

4 | DISCUSSION

Photosynthesis research has made huge progress in the last decades by fruitful combinations of biochemical, genetical, structural biological and biophysical approaches. Biophysical techniques have been crucial for understanding energy transfer and dissipation mechanisms. Especially ultrafast Chl time- and wavelength-resolved fluorescence spectroscopy in the femtosecond to nanosecond time range – combining the high time resolution with wavelength resolution - has provided

fundamental insights into photosynthetic processes (Chukhutsina et al., 2019; Croce and van Amerongen, 2020; Gilmore and Ball, 2000; Holzwarth, 1986; Holzwarth et al., 1985, Holzwarth et al., 2009; Holzwarth and Jahns, 2014) but has remained a speciality technique. Yet, many advantages and information gains of these ultrafast techniques could be provided by simpler Chl fluorescence spectrometers once the wavelength dimension is added. This would in many cases even give an added advantage over ultrafast techniques. For example, photosynthetic adaptation and regulation processes can be followed directly on the time scale of milliseconds to minutes/hours. We describe here a Chl fluorescence spectrometer system that measures all fluorescence quantities in a 3D fashion incorporating wavelength resolution which overcomes decisive limitations of current commercial systems. The instrument is easy-to-operate and can be used in any photosynthesis lab. In combination with the provided advanced spectro-kinetic analysis software this allows to obtain novel insights into the functioning of intact photosynthetic organisms and tissues.

In this contribution, we describe the working-principle of a new instrument, demonstrate yet undiscovered differences in the Chl fluorescence properties at different wavelengths and describe how they vary among plant species and growth conditions. We present data from five plant species with different leaf characteristics and a culture of a green alga demonstrating the wide practical application possibilities. In addition to *A. thaliana* and *P. abies* discussed in the main figures, chlorophyll fluorescence data from *M. deliciosa*, hybrid aspen and *C. reinhardtii* have been presented in Figure S2 and S3. The technology bears potential to be further developed to allow e.g. for identification of specific plant stress factors even by non-experts outside research laboratories.

The data allows for application of sophisticated methods for global spectro-kinetic data analysis. This in turn allows for decomposition into the underlying components providing basic functional insights into processes. We decompose the NPQ processes by a five-component intermediate and product reaction scheme. These five species are distinguished both by their different time developments and emission spectra. The analysis not only provides the kinetics (time courses) and the different spectral shapes, but the decomposed spectra contain additional information. We also describe some additional advantages with the technology like the STF approach that does not exceed the applied actinic light dose circumventing a problem with MTF techniques, the difference function to the FI'(t) signal. Moreover, during fluorescence induction experiments the quantum yield of PSII and wavelength-dependent contributions of PS I fluorescence can be better quantified (data not shown). The power of this methodology will become particularly apparent when employed on mutants lacking key proteins/processes and/or plants grown under different conditions. A detailed discussion and interpretation of this is beyond the scope of this contribution but is the subject of current work but we expect that, with the instrument now commercially available, such studies will follow in the near future.

Chl fluorescence spectrometry is already now a highly valuable tool for crop growth control and surveillance in greenhouses and in the fieldplant growers, for forest management and for environmental protection agencies. Adding wavelength resolution will become an important complement to current commercial fluorimeters increasing the possibilities for early identification of specific abiotic and biotic stress factors. With new instruments this technology will not be more complex in handling than current fluorescence spectrometers and could therefore be employed by non-experts in agriculture, greenhouses growth optimization, plant phenotyping, and environmental monitoring.

AUTHOR CONTRIBUTIONS

SN performed most of the measurements and downstream analyses, TS performed many of the measurements and, in particular, spectrokinetic analyses, MC performed some measurements and analyses, CH, BS, TdB, RB, LvdG, FH, PL, RL, VM, WJN, MR, RP, BS and IHMvS participated to the construction and development of ChloroSpec, PB took part in data interpretation, SJ and ARH designed the study and ARH supervised design, analysis and interpretations. All authors contributed to the writing of the manuscript.

ACKNOWLEDGEMENTS

We want to express our gratitude to Prof. Croce for her hospitality and the extensive logistical and financial support provided over the years it took to develop ChloroSpec. We also thank Sonali S. Ranade for providing *P. abies* samples.

FUNDING INFORMATION

The development of ChloroSpec was funded by the Biophysics of Photosynthesis group of Prof. Roberta Croce (VU Amsterdam) with contributions from the Demonstrator Lab Amsterdam and the Dutch Organization for Scientific Research (NWO) through a Take-off grant to Prof. Croce. This research was also supported by funding from the Swedish Research Council VR, Kempestiftelserna, Swedish Foundation for Strategic Research (SSF) and Knut and Alice Wallenberg foundation to SJ and Human frontiers Long-term Fellowship to PB.

CONFLICT OF INTEREST STATEMENT

ARH is cofounder of Chlorospec B.V.

DATA AVAILABILITY STATEMENT

The data that support the findings of this study are available from the corresponding author upon reasonable request.

ORCID

Sanchali Nanda https://orcid.org/0000-0002-6694-7235
Tatyana Shutova https://orcid.org/0000-0002-4095-9609
Stefan Jansson https://orcid.org/0000-0002-7906-6891

REFERENCES

Bąba, W., Kompała-Bąba, A., Zabochnicka-Świątek, M., Luźniak, J., Hanczaruk, R., Adamski, A., Kalaji, H.M., 2019. Discovering trends in photosynthesis using modern analytical tools:More than 100 reasons to use chlorophyll fluorescence. *Photosynthetica* 57, 668–679. https://doi.org/10.32615/ps.2019.069

Bag, P., 2021. Light Harvesting in Fluctuating Environments: Evolution and Function of Antenna Proteins across Photosynthetic Lineage. *Plants Basel Switz.* 10, 1184. https://doi.org/10.3390/plants10061184

Bag, P., Chukhutsina, V., Zhang, Z., Paul, S., Ivanov, A.G., Shutova, T., Croce, R., Holzwarth, A.R., Jansson, S., 2020. Direct energy transfer from photosystem II to photosystem I confers winter sustainability in Scots Pine. *Nat. Commun.* 11, 6388. https://doi.org/10.1038/s41467-020-20137-9

Baker, N.R., 2008. Chlorophyll Fluorescence: A Probe of Photosynthesis In Vivo. *Annu. Rev. Plant Biol.* 59, 89–113. https://doi.org/10.1146/annurev.arplant.59.032607.092759

Baker, N.R., Oxborough, K., 2004. Chlorophyll Fluorescence as a Probe of Photosynthetic Productivity, in: Papageorgiou, G.C., Govindjee (Eds.), *Chlorophyll a Fluorescence: A Signature of Photosynthesis, Advances in Photosynthesis and Respiration*. SpringerNetherlands, Dordrecht, pp. 65–82.

Beechem, J.M., Ameloot, M., Brand, L., 1985. Global and Target Analysis of Complex Decay Phenomena. *Instrum. Sci. Technol.* 14, 379–402. https://doi.org/10.1080/10739148508543585

Berger, K., Machwitz, M., Kycko, M., Kefauver, S.C., Van Wittenberghe, S., Gerhards, M., Verrelst, J., Atzberger, C., van der Tol, C., Damm, A., Rascher, U., Herrmann, I., Paz, V.S., Fahrner, S., Pieruschka, R., Prikaziuk, E., Buchaillot, Ma.L., Halabuk, A., Celesti, M., Koren, G., Gormus, E.T., Rossini, M., Foerster, M., Siegmann, B., Abdelbaki, A., Tagliabue, G., Hank, T., Darvishzadeh, R., Aasen, H., Garcia, M., Pôças, I., Bandopadhyay, S., Sulis, M., Tomelleri, E., Rozenstein, O., Filchev, L., Stancile, G., Schlerf, M., 2022. Multi-sensor spectral synergies for crop stress detection and monitoring in the optical domain: A review. *Remote Sens. Environ.* 280, 113198. https://doi.org/10.1016/j.rse.2022.113198

Chaerle, L., Lenk, S., Leinonen, I., Jones, H.G., Van Der Straeten, D., Buschmann, C., 2009. Multi-sensor plant imaging: Towards the development of a stress-catalogue. *Biotechnol. J.* 4, 1152–1167. https://doi.org/10.1002/biot.200800242

Chukhutsina, V.U., Holzwarth, A.R., Croce, R., 2019. Time-resolved fluorescence measurements on leaves: principles and recent developments. *Photosynth. Res.* 140, 355–369. https://doi.org/10.1007/s11120-018-0607-8

Croce, R., van Amerongen, H., 2020. Light harvesting in oxygenic photosynthesis: Structural biology meets spectroscopy. *Science* 369. https://doi.org/10.1126/science.aay2058

Genty, B., Briantais, J.-M., Baker, N.R., 1989. The relationship between the quantum yield of photosynthetic electron transport and quenching of chlorophyll fluorescence. *Biochim. Biophys. Acta BBA - Gen. Subj.* 990, 87–92. https://doi.org/10.1016/S0304-4165(89)80016-9

Gilmore, A.M., Ball, M.C., 2000. Protection and storage of chlorophyll in overwintering evergreens. *Proc. Natl. Acad. Sci. U. S. A.* 97, 11098–11101.

Golub, G., Pereyra, V., 2003. Separable nonlinear least squares: the variable projection method and its applications. *Inverse Probl.* 19, R1. https://doi.org/10.1088/0266-5611/19/2/201

Gorbunov, M.Y., Falkowski, P.G., 2022. Using Chlorophyll Fluorescence to Determine the Fate of Photons Absorbed by Phytoplankton in the World's Oceans. *Annu. Rev. Mar. Sci.* 14, 213–238. https://doi.org/10.1146/annurev-marine-032621-122346

Guidi, L., Degl'Innocenti, E., 2012. Chlorophyll a Fluorescence in Abiotic Stress, in: Venkateswarlu, B., Shanker, A.K., Shanker, C., Maheswari, M. (Eds.), *Crop Stress and Its Management: Perspectives and Strategies*. SpringerNetherlands, Dordrecht, pp. 359–398. https://doi.org/10.1007/978-94-007-2220-0_10

Holzwarth, A.R., 1996. Data Analysis of Time-Resolved Measurements, in: Amesz, J., Hoff, A.J. (Eds.), *Biophysical Techniques in Photosynthesis, Advances in Photosynthesis and Respiration*. SpringerNetherlands, Dordrecht, pp. 75–92.

Holzwarth, A.R., 1986. Fluorescence Lifetimes in Photosynthetic Systems. *Photochem. Photobiol.* 43, 707–725. https://doi.org/10.1111/j.1751-1097.1986.tb05650.x

Holzwarth, A.R., Jahns, P., 2014. Non-Photochemical Quenching Mechanisms in Intact Organisms as Derived from Ultrafast-Fluorescence Kinetic Studies, in: Demmig-Adams, B., Garab, G., Adams III, W., Govindjee (Eds.), *Non-Photochemical Quenching and Energy Dissipation in Plants, Algae and Cyanobacteria, Advances in Photosynthesis and Respiration*. SpringerNetherlands, Dordrecht, pp. 129–156.

Holzwarth, A.R., Lenk, D., Jahns, P., 2013. On the analysis of non-photochemical chlorophyll fluorescence quenching curves: I. Theoretical considerations. *Biochim. Biophys. Acta BBA - Bioenerg.* 1827, 786–792.

Holzwarth, A.R., Miloslavina, Y., Nilkens, M., Jahns, P., 2009. Identification of two quenching sites active in the regulation of photosynthetic light-harvesting studied by time-resolved fluorescence. *Chem. Phys. Lett.* 483, 262–267. https://doi.org/10.1016/j.cplett.2009.10.085

Holzwarth, A.R., Wendler, J., Haehnel, W., 1985. Time-resolved picosecond fluorescence spectra of the antenna chlorophylls in Chlorella vulgaris. Resolution of Photosystem I fluorescence. *Biochim. Biophys. Acta BBA - Bioenerg.* 807, 155–167. https://doi.org/10.1016/0005-2728(85)90119-7

Horton, P., Ruban, A.V., Walters, R.G., 1996. Regulation of Light Harvesting in Green Plants. *Annu. Rev. Plant Physiol. Plant Mol. Biol.* 47, 655–684. https://doi.org/10.1146/annurev.arplant.47.1.655

Johnson, X., Vandystadt, G., Bujaldon, S., Wollman, F.-A., Dubois, R., Roussel, P., Alric, J., Béal, D., 2009. A new setup for in vivo fluorescence imaging of photosynthetic activity. *Photosynth. Res.* 102, 85–93. https://doi.org/10.1007/s11120-009-9487-2

Kalaji, H.M., Schansker, G., Brestic, M., Bussotti, F., Calatayud, A., Ferroni, L., Goltsev, V., Guidi, L., Jajoo, A., Li, P., Losciale, P., Mishra, V.K., Misra, A.N., Nebauer, S.G., Pancaldi, S., Penella, C., Pollastrini, M., Suresh, K., Tambussi, E., Yanniccari, M., Zivcak, M., Cetner, M.D., Samborska, I.A., Stirbet, A., Olsovska, K., Kunderlikova, K., Shelonzek, H., Rusinowski, S., Bąba, W., 2017. Frequently asked questions about chlorophyll fluorescence, the sequel. *Photosynth. Res.* 132, 13–66. https://doi.org/10.1007/s11120-016-0318-y

Kalaji, H.M., Schansker, G., Ladle, R.J., Goltsev, V., Bosa, K., Allakhverdiev, S.I., Brestic, M., Bussotti, F., Calatayud, A., Dąbrowski, P., Elsheery, N.I., Ferroni, L., Guidi, L., Hogewoning, S.W., Jajoo, A., Misra, A.N., Nebauer, S.G., Pancaldi, S., Penella, C., Poli, D., Pollastrini, M., Romanowska-Duda, Z.B., Rutkowska, B., Serôdio, J., Suresh, K., Szulc, W., Tambussi, E., Yanniccari, M., Zivcak, M., 2014. Frequently asked questions about in vivo chlorophyll fluorescence: practical issues. *Photosynth. Res.* 122, 121–158. https://doi.org/10.1007/s11120-014-0024-6

Kaňa, R., Prášil, O., Komárek, O., Papageorgiou, G.C., Govindjee, 2009. Spectral characteristic of fluorescence induction in a model cyanobacterium, Synechococcus sp. (PCC 7942). *Biochim. Biophys. Acta BBA - Bioenerg.* 1787, 1170–1178. https://doi.org/10.1016/j.bbabio.2009.04.013

Kautsky, H., Hirsch, A., 1931. Neue Versuche zur Kohlensaeureassimilation. *Naturwissenschaften* 19, 964–964. https://doi.org/10.1007/BF01516164

Lichtenthaler, H.K., 2021. Multi-colour fluorescence imaging of photosynthetic activity and plant stress. *Photosynthetica* 59, 364–380. https://doi.org/10.32615/ps.2021.020

Malnoë, A., 2018. Photoinhibition or photoprotection of photosynthesis? Update on the (newly termed) sustained quenching component qH. *Environ. Exp. Bot., An Integrative Approach to Photoinhibition and Photoprotection of Photosynthesis* 154, 123–133. https://doi.org/10.1016/j.envexpbot.2018.05.005

Minagawa, J., 2013. Dynamic reorganization of photosynthetic supercomplexes during environmental acclimation of photosynthesis. *Front. Plant Sci.* 4.

Moustakas, M., Calatayud, Á., Guidi, L., 2021. Editorial: Chlorophyll Fluorescence Imaging Analysis in Biotic and Abiotic Stress. *Front. Plant Sci.* 12, 658500. https://doi.org/10.3389/fpls.2021.658500

Nedbal, L., Whitmarsh, J., 2004. Chlorophyll Fluorescence Imaging of Leaves and Fruits, in: Papageorgiou, G.C., Govindjee (Eds.),

Chlorophyll a Fluorescence: A Signature of Photosynthesis, *Advances in Photosynthesis and Respiration*. SpringerNetherlands, Dordrecht, pp. 389–407.

Pérez-Bueno, M.L., Pineda, M., Barón, M., 2019. Phenotyping plant responses to biotic stress by chlorophyll fluorescence imaging. *Front. Plant Sci.* 10, 1135.

Pfündel, E.E., 2021. Simultaneously measuring pulse-amplitude-modulated (PAM) chlorophyll fluorescence of leaves at wavelengths shorter and longer than 700 nm. *Photosynth. Res.* 147, 345–358. https://doi.org/10.1007/s11120-021-00821-7

Pieruschka, R., Klimov, D., Berry, J.A., Osmond, C.B., Rascher, U., Kolber, Z.S., 2012. Remote Chlorophyll Fluorescence Measurements with the Laser-Induced Fluorescence Transient Approach, in: Normanly, J. (Ed.), *High-Throughput Phenotyping in Plants: Methods and Protocols*, *Methods in Molecular Biology*. Humana Press, Totowa, NJ, pp. 51–59.

Remelli, W., Santabarbara, S., 2018. Excitation and emission wavelength dependence of fluorescence spectra in whole cells of the cyanobacterium *Synechocystis sp*. PPC6803: Influence on the estimation of Photosystem II maximal quantum efficiency. *Biochim. Biophys. Acta BBA - Bioenerg.* 1859, 1207–1222. https://doi.org/10.1016/j.bbabio.2018.09.366

Rizzo, F., Zucchelli, G., Jennings, R., Santabarbara, S., 2014. Wavelength dependence of the fluorescence emission under conditions of open and closed Photosystem II reaction centres in the green alga *Chlorella sorokiniana*. *Biochim. Biophys. Acta BBA - Bioenerg.* 1837, 726–733. https://doi.org/10.1016/j.bbabio.2014.02.009

Roelofs, T.A., Lee, C.H., Holzwarth, A.R., 1992. Global target analysis of picosecond chlorophyll fluorescence kinetics from pea chloroplasts: A new approach to the characterization of the primary processes in photosystem II alpha- and beta-units. *Biophys. J.* 61, 1147–1163. https://doi.org/10.1016/s0006-3495(92)81924-0

Santabarbara, S., Remelli, W., Petrova, A.A., Casazza, A.P., Santabarbara, S., Remelli, W., Petrova, A.A., Casazza, A.P., 2020. Influence of the Wavelength of Excitation and Fluorescence Emission Detection on the Estimation of Fluorescence-Based Physiological Parameters in Different Classes of Photosynthetic Organisms, in: Fluorescence Methods for Investigation of Living Cells and Microorganisms. *IntechOpen*. https://doi.org/10.5772/intechopen.93230

Santabarbara, S., Villafiorita Monteleone, F., Remelli, W., Rizzo, F., Menin, B., Casazza, A.P., 2019. Comparative excitation-emission dependence of the FV /FM ratio in model green algae and cyanobacterial strains. *Physiol. Plant.* 166, 351–364. https://doi.org/10.1111/ppl.12931

Schansker, G., Tóth, S.Z., Holzwarth, A.R., Garab, G., 2014. Chlorophyll a fluorescence: beyond the limits of the QA model. *Photosynth. Res.* 120, 43–58. https://doi.org/10.1007/s11120-013-9806-5

Schreiber, U., Schliwa, U., Bilger, W., 1986. Continuous recording of photochemical and non-photochemical chlorophyll fluorescence quenching with a new type of modulation fluorometer. *Photosynth. Res.* 10, 51–62. https://doi.org/10.1007/BF00024185

Stirbet, A., Govindjee, 2011. On the relation between the Kautsky effect (chlorophyll a fluorescence induction) and Photosystem II: Basics and applications of the OJIP fluorescence transient. J. Photochem. Photobiol. *B, Special Issue on Recent Progress in the Studies of Structure and Function of Photosystem II* 104, 236–257. https://doi.org/10.1016/j.jphotobiol.2010.12.010

Strasser, R.J., Srivastava, A., Tsimilli-Michael, M., 2000. The fluorescence transient as a tool to characterize and screen photosynthetic samples. *Probing Photosynth. Mech. Regul. Adapt.* 445–483.

Sun, D., Robbins, K., Morales, N., Shu, Q., Cen, H., 2022. Advances in optical phenotyping of cereal crops. *Trends Plant Sci.* 27, 191–208. https://doi.org/10.1016/j.tplants.2021.07.015

Sun, Y., Wen, J., Gu, L., Joiner, J., Chang, C.Y., van der Tol, C., Porcar-Castell, A., Magney, T., Wang, L., Hu, L., Rascher, U., Zarco-Tejada, P., Barrett, C.B., Lai, J., Han, J., Luo, Z., 2023. From remotely-sensed solar-induced chlorophyll fluorescence to ecosystem structure, function, and service: Part II—Harnessing data. *Glob. Change Biol.* 29, 2893–2925. https://doi.org/10.1111/gcb.16646

van Stokkum, I.H.M., Larsen, D.S., van Grondelle, R., 2004. Global and target analysis of time-resolved spectra. *Biochim. Biophys. Acta BBA - Bioenerg.* 1657, 82–104. https://doi.org/10.1016/j.bbabio.2004.04.011

Wientjes, E., Philippi, J., Borst, J.W., van Amerongen, H., 2017. Imaging the Photosystem I/Photosystem II chlorophyll ratio inside the leaf. *Biochim. Biophys. Acta Bioenerg.* 1858, 259–265. https://doi.org/10.1016/j.bbabio.2017.01.008

Zavafer, A., Labeeuw, L., Mancilla, C., 2020. Global Trends of Usage of Chlorophyll Fluorescence and Projections for the Next Decade. *Plant Phenomics* 2020. https://doi.org/10.34133/2020/6293145

SUPPORTING INFORMATION

Additional supporting information can be found online in the Supporting Information section at the end of this article.

How to cite this article: Nanda, S., Shutova, T., Cainzos, M., Hu, C., Sasbrink, B., Bag, P. et al. (2024) *ChloroSpec*: A new *in vivo* chlorophyll fluorescence spectrometer for simultaneous wavelength- and time-resolved detection. *Physiologia Plantarum*, 176(2), e14306. Available from: https://doi.org/10.1111/ppl.14306